



Article scientifique

Article

2000

Published version

Open Access

This is the published version of the publication, made available in accordance with the publisher's policy.

Search for Scalar Top and Scalar Bottom Quarks in pp Collisions at
 $s\sqrt{=}1.8\text{TeV}$

Collaborators: Clark, Allan Geoffrey; Kambara, Hisanori; Speer, Thomas; Strumia Michelini, Federica; Wu, Xin

How to cite

CDF Collaboration. Search for Scalar Top and Scalar Bottom Quarks in pp Collisions at $s\sqrt{=}1.8\text{TeV}$. In: Physical review letters, 2000, vol. 84, n° 25, p. 5704–5709. doi: 10.1103/PhysRevLett.84.5704

This publication URL: <https://archive-ouverte.unige.ch/unige:37874>

Publication DOI: [10.1103/PhysRevLett.84.5704](https://doi.org/10.1103/PhysRevLett.84.5704)

Search for Scalar Top and Scalar Bottom Quarks in $p\bar{p}$ Collisions at $\sqrt{s} = 1.8$ TeV

T. Affolder,²¹ H. Akimoto,⁴³ A. Akopian,³⁶ M. G. Albrow,¹⁰ P. Amaral,⁷ S. R. Amendolia,³² D. Amidei,²⁴ K. Anikeev,²² J. Antos,¹ G. Apollinari,³⁶ T. Arisawa,⁴³ T. Asakawa,⁴¹ W. Ashmanskas,⁷ M. Atac,¹⁰ F. Azfar,²⁹ P. Azzi-Bacchetta,³⁰ N. Bacchetta,³⁰ M. W. Bailey,²⁶ S. Bailey,¹⁴ P. de Barbaro,³⁵ A. Barbaro-Galtieri,²¹ V. E. Barnes,³⁴ B. A. Barnett,¹⁷ M. Barone,¹² G. Bauer,²² F. Bedeschi,³² S. Belforte,⁴⁰ G. Bellettini,³² J. Bellinger,⁴⁴ D. Benjamin,⁹ J. Bensinger,⁴ A. Beretvas,¹⁰ J. P. Berge,¹⁰ J. Berryhill,⁷ S. Bertolucci,¹² B. Bevensee,³¹ A. Bhatti,³⁶ C. Bigongiari,³² M. Binkley,¹⁰ D. Bisello,³⁰ R. E. Blair,² C. Blocker,⁴ K. Bloom,²⁴ B. Blumenfeld,¹⁷ B. S. Blusk,³⁵ A. Bocci,³² A. Bodek,³⁵ W. Bokhari,³¹ G. Bolla,³⁴ Y. Bonushkin,⁵ D. Bortoletto,³⁴ J. Boudreau,³³ A. Brandl,²⁶ S. van den Brink,¹⁷ C. Bromberg,²⁵ M. Brozovic,⁹ N. Bruner,²⁶ E. Buckley-Geer,¹⁰ J. Budagov,⁸ H. S. Budd,³⁵ K. Burkett,¹⁴ G. Busetto,³⁰ A. Byon-Wagner,¹⁰ K. L. Byrum,² M. Campbell,²⁴ A. Caner,³² W. Carithers,²¹ J. Carlson,²⁴ D. Carlsmith,⁴⁴ J. Cassada,³⁵ A. Castro,³⁰ D. Cauz,⁴⁰ A. Cerri,³² A. W. Chan,¹ P. S. Chang,¹ P. T. Chang,¹ J. Chapman,²⁴ C. Chen,³¹ Y. C. Chen,¹ M.-T. Cheng,¹ M. Chertok,³⁸ G. Chiarelli,³² I. Chirikov-Zorin,⁸ G. Chlachidze,⁸ F. Chlebana,¹⁰ L. Christofek,¹⁶ M. L. Chu,¹ S. Cihangir,¹⁰ C. I. Ciobanu,²⁷ A. G. Clark,¹³ M. Cobal,³² E. Cocca,³² A. Connolly,²¹ J. Conway,³⁷ J. Cooper,¹⁰ M. Cordelli,¹² D. Costanzo,³² J. Cranshaw,³⁹ D. Cronin-Hennessy,⁹ R. Cropp,²³ R. Culbertson,⁷ D. Dagenhart,⁴² F. DeJongh,¹⁰ S. Dell'Agnello,¹² M. Dell'Orso,³² R. Demina,¹⁰ L. Demortier,³⁶ M. Deninno,³ P. F. Derwent,¹⁰ T. Devlin,³⁷ J. R. Dittmann,¹⁰ S. Donati,³² J. Done,³⁸ T. Dorigo,¹⁴ N. Eddy,¹⁶ K. Einsweiler,²¹ J. E. Elias,¹⁰ E. Engels Jr.,³³ W. Erdmann,¹⁰ D. Errede,¹⁶ S. Errede,¹⁶ Q. Fan,³⁵ R. G. Feild,⁴⁵ C. Ferretti,³² I. Fiori,³ B. Flaughner,¹⁰ G. W. Foster,¹⁰ M. Franklin,¹⁴ J. Freeman,¹⁰ J. Friedman,²² Y. Fukui,²⁰ S. Galeotti,³² M. Gallinaro,³⁶ T. Gao,³¹ M. Garcia-Sciveres,²¹ A. F. Garfinkel,³⁴ P. Gatti,³⁰ C. Gay,⁴⁵ S. Geer,¹⁰ D. W. Gerdes,²⁴ P. Giannetti,³² P. Giromini,¹² V. Glagolev,⁸ M. Gold,²⁶ J. Goldstein,¹⁰ A. Gordon,¹⁴ A. T. Goshaw,⁹ Y. Gorta,³³ K. Goulianos,³⁶ H. Grassmann,⁴⁰ C. Green,³⁴ L. Groer,³⁷ C. Grosso-Pilcher,⁷ M. Guenther,³⁴ G. Guillian,²⁴ J. Guimaraes da Costa,²⁴ R. S. Guo,¹ C. Haber,²¹ E. Hafen,²² S. R. Hahn,¹⁰ C. Hall,¹⁴ T. Handa,¹⁵ R. Handler,⁴⁴ W. Hao,³⁹ F. Happacher,¹² K. Hara,⁴¹ A. D. Hardman,³⁴ R. M. Harris,¹⁰ F. Hartmann,¹⁸ K. Hatakeyama,³⁶ J. Hauser,⁵ J. Heinrich,³¹ A. Heiss,¹⁸ B. Hinrichsen,²³ K. D. Hoffman,³⁴ C. Holck,³¹ R. Hollebeek,³¹ L. Holloway,¹⁶ R. Hughes,²⁷ J. Huston,²⁵ J. Huth,¹⁴ H. Ikeda,⁴¹ M. Incagli,³² J. Incandela,¹⁰ G. Introzzi,³² J. Iwai,⁴³ Y. Iwata,¹⁵ E. James,²⁴ H. Jensen,¹⁰ M. Jones,³¹ U. Joshi,¹⁰ H. Kambara,¹³ T. Kamon,³⁸ T. Kaneko,⁴¹ K. Karr,⁴² H. Kasha,⁴⁵ Y. Kato,²⁸ T. A. Keaffaber,³⁴ K. Kelley,²² M. Kelly,²⁴ R. D. Kennedy,¹⁰ R. Kephart,¹⁰ D. Khazins,⁹ T. Kikuchi,⁴¹ M. Kirk,⁴ B. J. Kim,¹⁹ H. S. Kim,¹⁶ M. J. Kim,¹⁹ S. H. Kim,⁴¹ Y. K. Kim,²¹ L. Kirsch,⁴ S. Klimenko,¹¹ D. Knoblauch,¹⁸ P. Koehn,²⁷ A. Königeter,¹⁸ K. Kondo,⁴³ J. Konigsberg,¹¹ K. Kordas,²³ A. Korn,²² A. Korytov,¹¹ E. Kovacs,² J. Kroll,³¹ M. Kruse,³⁵ S. E. Kuhlmann,² K. Kurino,¹⁵ T. Kuwabara,⁴¹ A. T. Laasanen,³⁴ N. Lai,⁷ S. Lami,³⁶ S. Lammel,¹⁰ J. I. Lamoureux,⁴ M. Lancaster,²¹ G. Latino,³² T. LeCompte,² A. M. Lee IV,⁹ S. Leone,³² J. D. Lewis,¹⁰ M. Lindgren,⁵ T. M. Liss,¹⁶ J. B. Liu,³⁵ Y. C. Liu,¹ N. Lockyer,³¹ J. Loken,²⁹ M. Loretì,³⁰ D. Lucchesi,³⁰ P. Lukens,¹⁰ S. Lusin,⁴⁴ L. Lyons,²⁹ J. Lys,²¹ R. Madrak,¹⁴ K. Maeshima,¹⁰ P. Maksimovic,¹⁴ L. Malferrari,³ M. Mangano,³² M. Mariotti,³⁰ G. Martignon,³⁰ A. Martin,⁴⁵ J. A. J. Matthews,²⁶ P. Mazzanti,³ K. S. McFarland,³⁵ P. McIntyre,³⁸ E. McKigney,³¹ M. Menguzzato,³⁰ A. Mezione,³² E. Meschi,³² C. Mesropian,³⁶ C. Miao,²⁴ T. Miao,¹⁰ R. Miller,²⁵ J. S. Miller,²⁴ H. Minato,⁴¹ S. Miscetti,¹² M. Mishina,²⁰ N. Moggi,³² E. Moore,²⁶ R. Moore,²⁴ Y. Morita,²⁰ A. Mukherjee,¹⁰ T. Muller,¹⁸ A. Munar,³² P. Murat,³² S. Murgia,²⁵ M. Musy,⁴⁰ J. Nachtman,⁵ S. Nahn,⁴⁵ H. Nakada,⁴¹ T. Nakaya,⁷ I. Nakano,¹⁵ C. Nelson,¹⁰ D. Neuberger,¹⁸ C. Newman-Holmes,¹⁰ C.-Y. P. Ngan,²² P. Nicolaidi,⁴⁰ H. Niu,⁴ L. Nodulman,² A. Nomerotski,¹¹ S. H. Oh,⁹ T. Ohmoto,¹⁵ T. Ohsugi,¹⁵ R. Oishi,⁴¹ T. Okusawa,²⁸ J. Olsen,⁴⁴ C. Pagliarone,³² F. Palmonari,³² R. Paoletti,³² V. Papadimitriou,³⁹ S. P. Pappas,⁴⁵ A. Parri,¹² D. Partos,⁴ J. Patrick,¹⁰ G. Pauletta,⁴⁰ M. Paulini,²¹ C. Paus,²² A. Perazzo,³² L. Pescara,³⁰ T. J. Phillips,⁹ G. Piacentino,³² K. T. Pitts,¹⁰ R. Plunkett,¹⁰ A. Pompos,³⁴ L. Pondrom,⁴⁴ G. Pope,³³ M. Popovic,²³ F. Prokoshin,⁸ J. Proudfoot,² F. Ptohos,¹² G. Punzi,³² K. Ragan,²³ A. Rakitine,²² D. Reher,²¹ A. Reichold,²⁹ W. Riegler,¹⁴ A. Ribon,³⁰ F. Rimondi,³ L. Ristori,³² W. J. Robertson,⁹ A. Robinson,²³ T. Rodrigo,⁶ S. Rolli,⁴² L. Rosenson,²² R. Roser,¹⁰ R. Rossin,³⁰ W. K. Sakumoto,³⁵ D. Saltzberg,⁵ A. Sansoni,¹² L. Santi,⁴⁰ H. Sato,⁴¹ P. Savard,²³ P. Schlabach,¹⁰ E. E. Schmidt,¹⁰ M. P. Schmidt,⁴⁵ M. Schmitt,¹⁴ L. Scodellaro,³⁰ A. Scott,⁵ A. Scribano,³² S. Segler,¹⁰ S. Seidel,²⁶ Y. Seiya,⁴¹ A. Semenov,⁸ F. Semeria,³ T. Shah,²² M. D. Shapiro,²¹ P. F. Shepard,³³ T. Shibayama,⁴¹ M. Shimojima,⁴¹ M. Shochet,⁷ J. Siegrist,²¹ G. Signorelli,³² A. Sill,³⁹ P. Sinervo,²³ P. Singh,¹⁶ A. J. Slaughter,⁴⁵ K. Sliwa,⁴² C. Smith,¹⁷ F. D. Snider,¹⁰ A. Solodsky,³⁶ J. Spalding,¹⁰ T. Speer,¹³ P. Sphicas,²² F. Spinella,³² M. Spiropulu,¹⁴ L. Spiegel,¹⁰ L. Stanco,³⁰

J. Steele,⁴⁴ A. Stefanini,³² J. Strolugas,¹⁶ F. Strumia,¹³ D. Stuart,¹⁰ K. Sumorok,²² T. Suzuki,⁴¹ R. Takashima,¹⁵ K. Takikawa,⁴¹ M. Tanaka,⁴¹ T. Takano,²⁸ B. Tannenbaum,⁵ W. Taylor,²³ M. Tecchio,²⁴ P. K. Teng,¹ K. Terashi,⁴¹ S. Tether,²² D. Theriot,¹⁰ R. Thurman-Keup,² P. Tipton,³⁵ S. Tkaczyk,¹⁰ K. Tollefson,³⁵ A. Tollestrup,¹⁰ H. Toyoda,²⁸ W. Trischuk,²³ J. F. de Troconiz,¹⁴ S. Truitt,²⁴ J. Tseng,²² N. Turini,³² F. Ukegawa,⁴¹ J. Valls,³⁷ S. Vejcik III,¹⁰ G. Velev,³² R. Vidal,¹⁰ R. Vilar,⁶ I. Vologouev,²¹ D. Vucinic,²² R. G. Wagner,² R. L. Wagner,¹⁰ J. Wahl,⁷ N. B. Wallace,³⁷ A. M. Walsh,³⁷ C. Wang,⁹ C. H. Wang,¹ M. J. Wang,¹ T. Watanabe,⁴¹ D. Waters,²⁹ T. Watts,³⁷ R. Webb,³⁸ H. Wenzel,¹⁸ W. C. Wester III,¹⁰ A. B. Wicklund,² E. Wicklund,¹⁰ H. H. Williams,³¹ P. Wilson,¹⁰ B. L. Winer,²⁷ D. Winn,²⁴ S. Wolbers,¹⁰ D. Wolinski,²⁴ J. Wolinski,²⁵ S. Worm,²⁶ X. Wu,¹³ J. Wyss,³² A. Yagil,¹⁰ W. Yao,²¹ G. P. Yeh,¹⁰ P. Yeh,¹ J. Yoh,¹⁰ C. Yosef,²⁵ T. Yoshida,²⁸ I. Yu,¹⁹ S. Yu,³¹ A. Zanetti,⁴⁰ F. Zetti,²¹ and S. Zucchelli³

(CDF Collaboration)

¹*Institute of Physics, Academia Sinica, Taipei, Taiwan 11529, Republic of China*

²*Argonne National Laboratory, Argonne, Illinois 60439*

³*Istituto Nazionale di Fisica Nucleare, University of Bologna, I-40127 Bologna, Italy*

⁴*Brandeis University, Waltham, Massachusetts 02254*

⁵*University of California at Los Angeles, Los Angeles, California 90024*

⁶*Instituto de Fisica de Cantabria, University of Cantabria, 39005 Santander, Spain*

⁷*Enrico Fermi Institute, University of Chicago, Chicago, Illinois 60637*

⁸*Joint Institute for Nuclear Research, RU-141980 Dubna, Russia*

⁹*Duke University, Durham, North Carolina 27708*

¹⁰*Fermi National Accelerator Laboratory, Batavia, Illinois 60510*

¹¹*University of Florida, Gainesville, Florida 32611*

¹²*Laboratori Nazionali di Frascati, Istituto Nazionale di Fisica Nucleare, I-00044 Frascati, Italy*

¹³*University of Geneva, CH-1211 Geneva 4, Switzerland*

¹⁴*Harvard University, Cambridge, Massachusetts 02138*

¹⁵*Hiroshima University, Higashi-Hiroshima 724, Japan*

¹⁶*University of Illinois, Urbana, Illinois 61801*

¹⁷*The Johns Hopkins University, Baltimore, Maryland 21218*

¹⁸*Institut für Experimentelle Kernphysik, Universität Karlsruhe, 76128 Karlsruhe, Germany*

¹⁹*Korean Hadron Collider Laboratory, Kyungpook National University, Taegu, 702-701, Korea;*

Seoul National University, Seoul, 151-742, Korea;

and Sung Kyun Kwan University, Suwon, 440-746, Korea

²⁰*High Energy Accelerator Research Organization (KEK), Tsukuba, Ibaraki 305, Japan*

²¹*Ernest Orlando Lawrence Berkeley National Laboratory, Berkeley, California 94720*

²²*Massachusetts Institute of Technology, Cambridge, Massachusetts 02139*

²³*Institute of Particle Physics, McGill University, Montreal H3A 2T8, Canada*

and University of Toronto, Toronto M5S 1A7, Canada

²⁴*University of Michigan, Ann Arbor, Michigan 48109*

²⁵*Michigan State University, East Lansing, Michigan 48824*

²⁶*University of New Mexico, Albuquerque, New Mexico 87131*

²⁷*The Ohio State University, Columbus, Ohio 43210*

²⁸*Osaka City University, Osaka 588, Japan*

²⁹*University of Oxford, Oxford OX1 3RH, United Kingdom*

³⁰*Universita di Padova, Istituto Nazionale di Fisica Nucleare, Sezione di Padova, I-35131 Padova, Italy*

³¹*University of Pennsylvania, Philadelphia, Pennsylvania 19104*

³²*Istituto Nazionale di Fisica Nucleare, University and Scuola Normale Superiore of Pisa, I-56100 Pisa, Italy*

³³*University of Pittsburgh, Pittsburgh, Pennsylvania 15260*

³⁴*Purdue University, West Lafayette, Indiana 47907*

³⁵*University of Rochester, Rochester, New York 14627*

³⁶*Rockefeller University, New York, New York 10021*

³⁷*Rutgers University, Piscataway, New Jersey 08855*

³⁸*Texas A&M University, College Station, Texas 77843*

³⁹*Texas Tech University, Lubbock, Texas 79409*

⁴⁰*Istituto Nazionale di Fisica Nucleare, University of Trieste, Udine, Italy*

⁴¹*University of Tsukuba, Tsukuba, Ibaraki 305, Japan*

⁴²*Tufts University, Medford, Massachusetts 02155*

⁴³*Waseda University, Tokyo 169, Japan*

⁴⁴*University of Wisconsin, Madison, Wisconsin 53706*

⁴⁵*Yale University, New Haven, Connecticut 06520*
(Received 25 October 1999)

We have searched for direct pair production of scalar top and scalar bottom quarks in 88 pb^{-1} of $p\bar{p}$ collisions at $\sqrt{s} = 1.8 \text{ TeV}$ with the CDF detector. We looked for events with a pair of heavy flavor jets and missing energy, consistent with scalar top (bottom) quark decays to a charm (bottom) quark and a neutralino. The numbers of events that pass our selections show no significant deviation from standard model expectations. We compare our results to the next-to-leading order scalar quark production cross sections to exclude regions in scalar quark-neutralino mass parameter space.

PACS numbers: 12.60.Jv, 13.85.Rm, 14.80.Ly

Supersymmetry (SUSY) [1] assigns to every fermionic standard model (SM) particle a bosonic superpartner. Therefore, the SM quark helicity states q_L and q_R acquire scalar partners \tilde{q}_L and \tilde{q}_R . SUSY models usually predict that the masses of the first two generations of scalar quarks are approximately degenerate. The scalar top quark (\tilde{t}) mass, however, may be lower than that of the other scalar quarks due to a substantial Yukawa coupling resulting from the large top quark mass. In addition, mixing between \tilde{t}_L and \tilde{t}_R can cause a large splitting between the mass eigenstates \tilde{t}_1 and \tilde{t}_2 [2]. We note that many baryogenesis models require a light stop quark [3].

The bottom quark mass is much smaller than the top quark mass, therefore the effect of the Yukawa coupling on the scalar bottom quark (\tilde{b}) mass is small. However, in some regions of SUSY parameter space a large mixing between \tilde{b}_L and \tilde{b}_R can still occur, leading to a significant splitting between mass eigenstates and a low mass value for the lighter mass eigenstate (\tilde{b}_1) [4].

At the Tevatron, third generation scalar quarks are expected to be produced in pairs via gg fusion and $q\bar{q}$ annihilation. In this Letter, we describe two analyses looking for processes in a minimal supersymmetric standard model framework: (i) a scalar top analysis, searching for the process $p\bar{p} \rightarrow \tilde{t}_1\bar{\tilde{t}}_1 \rightarrow (c\tilde{\chi}_1^0)(\bar{c}\tilde{\chi}_1^0)$, and (ii) a scalar bottom analysis, searching for the process $p\bar{p} \rightarrow \tilde{b}_1\bar{\tilde{b}}_1 \rightarrow (b\tilde{\chi}_1^0)(\bar{b}\tilde{\chi}_1^0)$. We assume the lightest neutralino $\tilde{\chi}_1^0$ is the lightest supersymmetric particle and stable. This leads to experimental signatures with appreciable missing transverse energy. The decay $\tilde{t}_1 \rightarrow c\tilde{\chi}_1^0$, as in process (i), dominates via a one-loop diagram in the absence of flavor-changing neutral currents if $m_{\tilde{t}_1} < m_b + m_{\tilde{\chi}_1^\pm}$, $m_{\tilde{t}_1} < m_W + m_b + m_{\tilde{\chi}_1^0}$, $m_{\tilde{t}_1} < m_b + m_{\tilde{\nu}}$, and $m_{\tilde{t}_1} < m_b + m_{\tilde{l}}$ [2]. For process (ii) we assume $m_{\tilde{b}_1} > m_b + m_{\tilde{\chi}_1^0}$ and $m_{\tilde{b}_1} < m_b + m_{\tilde{\chi}_2^0}$ [4]. Here, $\tilde{\chi}_1^\pm$ and $\tilde{\chi}_2^0$ are the lightest chargino and next-to-lightest neutralino, $\tilde{\nu}$ and \tilde{l} are the scalar neutrino and scalar lepton. Therefore, the signature of both processes is a pair of acolinear heavy flavor jets, \cancel{E}_T , and no high P_T leptons in the final state.

We have searched data corresponding to a total integrated luminosity of $88.0 \pm 3.6 \text{ pb}^{-1}$ collected using the CDF detector during the 1994–1995 Tevatron run. CDF is a general purpose detector and is described in detail elsewhere [5]. Here we give a brief description of the components relevant to this analysis. The innermost

part of CDF, a four-layer silicon vertex detector (SVX'), allows a precise measurement of a track's impact parameter with respect to the primary vertex in the plane transverse to the beam direction [6]. A time projection chamber determines the position of the primary vertex along the beam direction. The central drift chamber, located inside a 1.4-T superconducting solenoidal magnet, measures the momenta of the charged particles. Outside the drift chamber there is a calorimeter, which is organized into electromagnetic and hadronic components, with projective towers covering the pseudorapidity range $|\eta| < 4.2$. The muon system is located outside the calorimeter and covers the range $|\eta| < 1$. Events for this analysis were collected using a trigger which required missing transverse energy $\cancel{E}_T > 35 \text{ GeV}$. \cancel{E}_T is the energy imbalance in the directions transverse to the beam direction using the raw energy deposited in calorimeter towers with $|\eta| < 3.6$.

After removing events with large \cancel{E}_T from accelerator-induced and cosmic ray sources, we select events with two or three jets that have transverse energy $E_T \geq 15 \text{ GeV}$ and $|\eta| \leq 2$ (hard jets) and no additional jets with $E_T \geq 7 \text{ GeV}$ and $|\eta| \leq 3.6$ (mostly soft jets). These requirements efficiently reject $t\bar{t}$ events (which have more than 3 hard jets) and QCD multijet events (which have soft jets due to gluon radiation). Jets are found from calorimeter information using a fixed cone algorithm [7] with a cone radius of 0.4 in η - ϕ and jet energies are calculated using the raw energy deposition in calorimeter towers. The angle ϕ is the angle in the plane normal to the beam direction. To reduce systematic effects from the trigger, we require events to have $\cancel{E}_T > 40 \text{ GeV}$, and to reject events with fake missing energy arising from jet energy mismeasurements we require that the missing transverse energy direction is neither parallel to any jet (j) nor antiparallel to the leading E_T jet: $\Delta\phi(\cancel{E}_T, j) > 45^\circ$ and $\Delta\phi(\cancel{E}_T, j_1) < 165^\circ$ where the jet indices are ordered by decreasing E_T . Moreover, to reduce the QCD background, we require the angle between the two leading jets to be $45^\circ < \Delta\phi(j_1, j_2) < 165^\circ$. We reject events with one or more identified electrons (muons) with $E_T(P_T) > 10 \text{ GeV}$ (GeV/c).

After applying these requirements, the data sample (which we call the pretag sample) contains 396 events. The largest source of background in the pretag sample is the production of W + jets, where the W decays to a neutrino (leading to missing energy) and either an electron

or muon that is not identified or a tau which decays hadronically.

The SVX' information is used to tag heavy-flavor jets. We associate tracks to a jet by requiring that the track be within a cone of 0.4 in η - ϕ space around the jet axis. We require tracks to have $P_T > 1.0$ GeV/ c , positive impact parameter, and a good SVX' hit pattern. A good SVX' hit pattern consists of three or four hits in the SVX' detector with no hits shared by other tracks. We take the sign of a track's impact parameter to be the sign of the scalar product of the impact parameter and jet E_T vectors. We then define the impact parameter significance to be the impact parameter divided by its uncertainty. For tracks originating from the primary vertex the impact parameter significance distribution is symmetric around zero with a shape determined by the SVX' resolution, while decay products of long lived objects tend to have large positive impact parameter significances. We therefore use the negative impact parameter significance distribution to define the detector resolution function. For each track, we determine the probability that the track comes from the primary vertex using this resolution function. We call this probability *track probability*. By construction, the *track probability* distribution is flat for tracks originating from the primary vertex, and peaks near zero for tracks from a secondary vertex. We combine the track probabilities for all tracks associated to a jet to form the *jet probability* (\mathcal{P}_{jet}) [8], the probability that all the tracks in the jet come from the primary vertex. The distribution of \mathcal{P}_{jet} is flat for jets originating from the primary vertex by construction, while for bottom and charm jets it peaks near zero.

We select events for the scalar top analysis by requiring the event to have at least one taggable jet with a $\mathcal{P}_{\text{jet}} \leq 0.05$. A taggable jet has at least two SVX' tracks as defined above. The distribution of the minimum jet probability ($\mathcal{P}_{\text{jet}}^{\text{min}}$) of the taggable jets in the pretag sample is shown in Fig. 1. This requirement, chosen to optimize the expected signal significance, rejects approximately 97% of the background while its efficiency for the signal is 25%. For the scalar bottom analysis the expected signal significance is optimized by requiring that the event has at least one taggable jet with a $\mathcal{P}_{\text{jet}}^{\text{min}} \leq 0.01$. This requirement rejects approximately 99% of the background while retaining 45% of the scalar bottom signal. The total scalar top (bottom) efficiencies in the accessible mass region vary from 0.1% (0.1%) to 3.2% (6.5%), the efficiencies increasing for higher scalar quark mass and larger mass difference between \tilde{t}_1 (\tilde{b}_1) and $\tilde{\chi}_1^0$.

Backgrounds (other than QCD multijet events) and the expected signal are estimated using a number of Monte Carlo programs followed by a full CDF detector simulation. Single vector boson production and decay is simulated using a tree-level calculation as implemented in the VECBOS [9] package, with HERWIG [10] routines used for subsequent parton hadronization. Vector boson pair production and decay is implemented in ISAJET [11]. Top

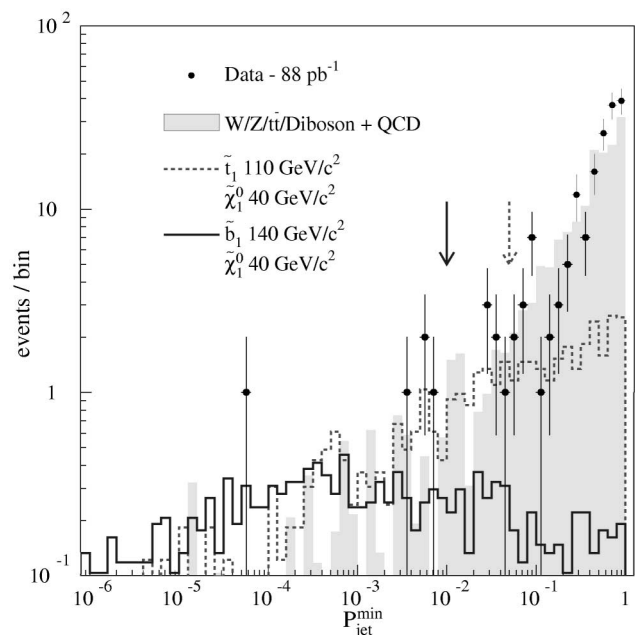


FIG. 1. The distribution of $\mathcal{P}_{\text{jet}}^{\text{min}}$ —the lowest value of \mathcal{P}_{jet} for all taggable jets in an event. A requirement of $\mathcal{P}_{\text{jet}}^{\text{min}} \leq 0.05(0.01)$ applied to select charm (bottom) jets is indicated by arrows. Points are data, the shaded histogram is the sum of the predicted backgrounds, the dashed line is the predicted signal for $m_{\tilde{t}_1} = 110$ GeV/ c^2 , $m_{\tilde{\chi}_1^0} = 40$ GeV/ c^2 , and the solid line is the predicted signal for $m_{\tilde{b}_1} = 140$ GeV/ c^2 , $m_{\tilde{\chi}_1^0} = 40$ GeV/ c^2 . The background and signal are normalized to 88 pb $^{-1}$.

pair production and decay is simulated using HERWIG. Signal events are modeled using the PYTHIA [12] generator. The PYTHIA Monte Carlo generator includes production and decay of SUSY particles [13]. The next-to-leading order (NLO) cross section for the scalar quark production is calculated using the PROSPINO [14] program with CTEQ3M parton distribution functions [15]. Simulated events are analyzed using the same procedure as the selected data sample. We check the single vector boson normalization with data by reversing the lepton veto requirement in the pretag sample.

We estimate the number of QCD multijet events in the tagged samples using a combination of Monte Carlo and data samples. We attribute the excess of data events above electroweak sources in the pretag data sample to QCD multijet sources. The total expected electroweak background in the pretag sample is 270.1 ± 76.2 which gives us an estimate of 125.9 ± 83.4 expected QCD multijet events in the pretag sample. We then apply a \mathcal{P}_{jet} mistag matrix to this excess to estimate the QCD multijet background after tagging. The \mathcal{P}_{jet} mistag matrix, which parametrizes the probability that a jet has $\mathcal{P}_{\text{jet}} \leq 0.05$ as a function of jet E_T and the number of SVX' tracks, is derived from data and verified in several control data samples.

The systematic uncertainties on the expected number of signal events apply for both \tilde{t}_1 and \tilde{b}_1 . The NLO cross section for third generation scalar quarks depends weakly on

TABLE I. The number of observed data and expected background events. For $W/Z/t\bar{t}$ /Diboson, the first uncertainty is statistical, the second is systematic. For QCD and Total Expected from SM, the uncertainty is statistical plus systematic.

Sample	$N_{\text{exp}} (\mathcal{P}_{\text{jet}}^{\text{min}} \leq 0.05)$	$N_{\text{exp}} (\mathcal{P}_{\text{jet}}^{\text{min}} \leq 0.01)$
$W^\pm(\rightarrow e^\pm \nu_e) + \geq 2$ jets	$0.3 \pm 0.3 \pm 0.1$...
$W^\pm(\rightarrow \mu^\pm \nu_\mu) + \geq 2$ jets	$0.9 \pm 0.5 \pm 0.3$...
$W^\pm(\rightarrow \tau^\pm \nu_\tau) + \geq 1$ jets	$7.6 \pm 1.6 \pm 2.2$	$3.0 \pm 1.0 \pm 0.9$
$Z^0(\rightarrow \nu\bar{\nu}) + \geq 2$ jets	$1.2 \pm 0.4 \pm 0.4$	$0.8 \pm 0.3 \pm 0.2$
$t\bar{t}$	$0.7 \pm 0.2 \pm 0.4$	$0.5 \pm 0.2 \pm 0.2$
Diboson(WW, WZ, ZZ)	$0.4 \pm 0.1 \pm 0.1$	$0.2 \pm 0.1 \pm 0.1$
Total $W/Z/t\bar{t}$ /Diboson	$11.1 \pm 1.8 \pm 3.3$	$4.5 \pm 1.1 \pm 1.2$
Total QCD	3.4 ± 1.7	1.3 ± 0.7
Total expected from SM	14.5 ± 4.2	5.8 ± 1.8
Total observed	11	5

other masses and parameters ($\sim 1\%$) [14]. The dominant NLO uncertainties are due to the choice of QCD renormalization scale (μ) and the choice of parton distribution function. The theoretical uncertainty on the NLO scalar quark production cross section is a function of the scalar quark mass and ranges from 11% to 22% for the mass range 30 to 150 GeV/c^2 . Gluon radiation from the initial state (ISR) or final state (FSR) partons is the largest source of systematic uncertainty. We determine its effect on our acceptance by turning off ISR or FSR in the signal Monte Carlo and comparing the efficiency with the default Monte Carlo which has ISR and FSR turned on. The combined ISR/FSR systematic uncertainty is 23%. We determine the jet energy systematic uncertainty, which is 10%, by varying the jet energies by $\pm 5\%$ [16]. The trigger efficiency systematic uncertainty, which is 10%, is determined by varying the trigger efficiency curve by $\pm 1\sigma$ of its fitted values. The detection efficiency estimates are derived from Monte Carlo that has exactly one primary vertex. The dominant effect of multiple primary vertices is to reduce the efficiency for a requirement of no extra jets with $E_T \geq 7$ GeV and $|\eta| \leq 3.6$. We account for the loss in efficiency due to the extra jet veto by combining the Monte Carlo with a minimum-bias data sample (consistent with the number of primary vertices found during the 1994–1995 Tevatron run), measuring the relative loss in efficiency and degrading the signal efficiency by this factor. The efficiency scale factor due to multiple primary vertices is 0.93 ± 0.03 . We use data samples enriched in charm (bottom) jets to determine the systematic uncertainty on the charm (bottom) tagging efficiency. The systematic uncertainty is 10% for both charm and bottom tagging. Including the systematic uncertainties due to the integrated luminosity measurement (4.1%) and finite Monte Carlo statistics (5%–15%), the total systematic varies from 31% to 36% as a function of the squark mass.

In the scalar top analysis we observe 11 events, which is consistent with 14.5 ± 4.2 events expected from SM processes (see Table I). We interpret the null result in the

scalar top search as an excluded region in $m_{\tilde{\chi}_1^0}$ - $m_{\tilde{t}_1}$ parameter space using a background subtraction method [17]. The 95% C.L. excluded region is shown in Fig. 2. The maximum $m_{\tilde{t}_1}$ excluded is 119 GeV/c^2 for $m_{\tilde{\chi}_1^0} = 40$ GeV/c^2 . The reach in $m_{\tilde{t}_1}$ is limited by the statistics, while the gap between the kinematic limit and the excluded region is mostly determined by the \cancel{E}_T cut which is effectively fixed by the \cancel{E}_T trigger threshold. Also shown in Fig. 2 are the results from the D0 experiment, based on 7.4 pb^{-1} [18], and from the OPAL experiment for $\sqrt{s} = 189$ GeV at LEP [19]. $\theta_{\tilde{t}}$ parametrizes the mixing of the left/right scalar bottom gauge eigenstates to form the light/heavy mass eigenstates. Note that the results for both D0 and CDF are independent of $\theta_{\tilde{t}}$.

In the scalar bottom analysis five events are observed with an expected background of 5.8 ± 1.8 (see Table I).

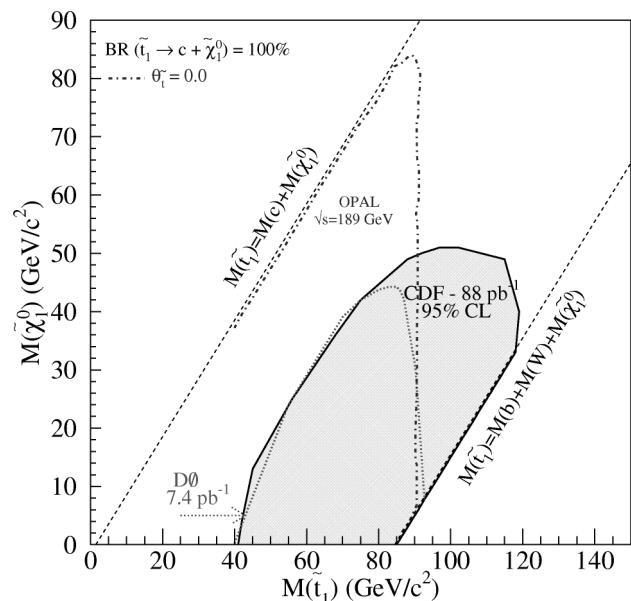


FIG. 2. 95% C.L. exclusion region (shaded region) in $m_{\tilde{\chi}_1^0}$ - $m_{\tilde{t}_1}$ plane for $\tilde{t}_1 \rightarrow c\tilde{\chi}_1^0$. See the text.

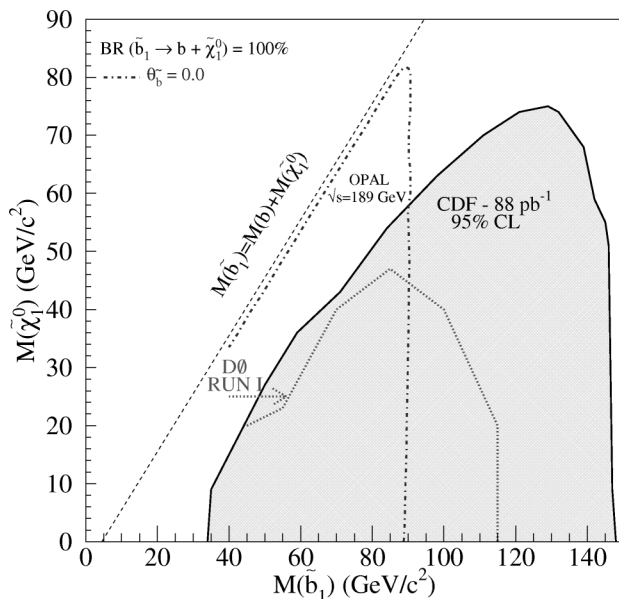


FIG. 3. 95% C.L. exclusion region (shaded region) in $m_{\tilde{\chi}_1^0}$ - $m_{\tilde{b}_1}$ plane for $\tilde{b}_1 \rightarrow b \tilde{\chi}_1^0$. See the text.

Similarly, we interpret the null result as an excluded region in $m_{\tilde{\chi}_1^0}$ - $m_{\tilde{b}_1}$ parameter space as shown in Fig. 3. For $m_{\tilde{\chi}_1^0} = 40$ GeV/ c^2 the maximum $m_{\tilde{b}_1}$ excluded is 146 GeV/ c^2 . Also plotted are the latest results from D0 [20] and OPAL [19].

In summary, we have performed a search for \tilde{t}_1/\tilde{b}_1 in $p\bar{p}$ collisions at $\sqrt{s} = 1.8$ TeV using 88 pb $^{-1}$ of data. We looked for events with significant missing energy, no high P_T lepton(s), and two or three jets. We required that at least one jet be consistent with originating from a heavy flavor jet using a technique called jet probability. After applying all selection criteria, we observed no excess of events above standard model predictions, and we set 95% C.L. exclusion regions in the $m_{\tilde{\chi}_1^0}$ - $m_{\tilde{q}_1}$ plane.

We thank the Fermilab staff and the technical staffs of the participating institutions for their vital contributions. This work was supported by the U.S. Department of Energy and National Science Foundation; the Italian Istituto Nazionale di Fisica Nucleare; the Ministry of Education, Science and Culture of Japan; the Natural Sciences and Engineering Research Council of Canada; the National

Science Council of the Republic of China; the A. P. Sloan Foundation; and the Swiss National Science Foundation.

- [1] For reviews of SUSY and the MSSM, see H. P. Nilles, Phys. Rep. **110**, 1 (1984); H. E. Haber and G. L. Kane, Phys. Rep. **117**, 75 (1985); S. P. Martin, hep-ph/9709356.
- [2] See, for example, K. Hikasa and M. Kobayashi, Phys. Rev. D **36**, 724 (1987); H. Baer *et al.*, Phys. Rev. D **44**, 725 (1991); H. Baer, J. Sender, and X. Tata, Phys. Rev. D **50**, 4517 (1994); R. Demina, J. Lykken, K. Matchev, and A. Nomerotski, hep-ph/9910275.
- [3] A. Riotto and M. Trodden, Annu. Rev. Nucl. Part. Sci. **49**, 35 (1999).
- [4] A. Bartl, W. Majerotto, and W. Porod, Z. Phys. C **64**, 499 (1994).
- [5] CDF Collaboration, F. Abe *et al.*, Nucl. Instrum. Methods Phys. Res., Sect. A **271**, 387 (1988); F. Abe *et al.*, Phys. Rev. D **50**, 2966 (1994).
- [6] CDF Collaboration, S. Cihangir *et al.*, Nucl. Instrum. Methods Phys. Res., Sect. A **360**, 137 (1995).
- [7] CDF Collaboration, F. Abe *et al.*, Phys. Rev. D **47**, 4857 (1993).
- [8] CDF Collaboration, F. Abe *et al.*, Phys. Rev. D **53**, 1051 (1996).
- [9] F. A. Berends, H. Kuijf, B. Tausk, and W. T. Giele, Nucl. Phys. **B357**, 32 (1991); W. T. Giele, E. W. Glover, and D. A. Kosower, Nucl. Phys. **B403**, 633 (1993).
- [10] G. Marchesini *et al.*, Comput. Phys. Commun. **67**, 465 (1992).
- [11] H. Baer, F. E. Paige, S. D. Protopopescu, and X. Tata, hep-ph/9305342.
- [12] T. Sjostrand, Comput. Phys. Commun. **82**, 74 (1994).
- [13] S. Mrenna, Comput. Phys. Commun. **101**, 232 (1997).
- [14] W. Beenakker *et al.*, Nucl. Phys. **B515**, 3 (1998).
- [15] CTEQ Collaboration, J. Huston *et al.*, Phys. Rev. D **51**, 6139 (1995).
- [16] CDF Collaboration, F. Abe *et al.*, Phys. Rev. Lett. **70**, 1376 (1993).
- [17] C. Caso *et al.*, Eur. Phys. J. **C3**, 176 (1998).
- [18] D0 Collaboration, S. Abachi *et al.*, Phys. Rev. Lett. **76**, 2222 (1996).
- [19] OPAL Collaboration, G. Abbiendi *et al.*, Phys. Lett. B **456**, 95 (1999).
- [20] D0 Collaboration, B. Abbott *et al.*, Phys. Rev. D **60**, 031101 (1999).